

# Optical Engineering

[SPIDigitalLibrary.org/oe](http://SPIDigitalLibrary.org/oe)

## **Fast-response liquid crystal variable optical retarder and multilevel attenuator**

HsienHui Cheng  
Achintya Bhowmik  
Philip J. Bos

# Fast-response liquid crystal variable optical retarder and multilevel attenuator

**HsienHui Cheng**

Kent State University  
Liquid Crystal Institute and Chemical Physics  
Interdisciplinary Program  
Kent, Ohio 44242

**Achintya Bhowmik**

Intel Corporation  
2200 Mission College Boulevard  
Santa Clara, California 95054

**Philip J. Bos**

Kent State University  
Liquid Crystal Institute and Chemical Physics  
Interdisciplinary Program  
Kent, Ohio 44242  
E-mail: [pbos@kent.edu](mailto:pbos@kent.edu)

**Abstract.** We propose and demonstrate a fast-response liquid crystal (LC) variable optical retarder or attenuator with several transmission levels. The fast-response LC optical device consists of dual  $\pi$ -cells. The device is designed so that the transition between any two states is controlled by the application of an increased voltage level rather than by applying a lower level. This design offers transition times in the range of tens of microseconds between any transmission states. A limitation of the device is that the time between transitions cannot be arbitrarily short and is typically milliseconds. © The Authors. Published by SPIE under a Creative Commons Attribution 3.0 Unported License. Distribution or reproduction of this work in whole or in part requires full attribution of the original publication, including its DOI. [DOI: [10.1117/1.OE.52.10.107105](https://doi.org/10.1117/1.OE.52.10.107105)]

Subject terms: fast-response optical shutter; variable retarder; optically compensated bend cell; three-dimensional display.

Paper 130668 received May 6, 2013; revised manuscript received Sep. 18, 2013; accepted for publication Sep. 24, 2013; published online Oct. 16, 2013.

## 1 Introduction

A fast-response liquid crystal (LC) optical retarder or an attenuator with multilevel transmission is needed for many applications, where LC devices are considered to be too slow [e.g., in the field of optical communications or for field sequential three-dimensional (3-D) displays of the future].

The response time of conventional nematic LC devices is usually in the range of milliseconds. Methods have been developed for faster response including polymer-stabilized LC,<sup>1-3</sup> polymer-dispersed LC,<sup>4</sup> and  $\pi$ -cells.<sup>5-8</sup> However, the transition time of all of these devices are still in the range of several milliseconds and not sufficient for the high-frame rates needed for multifield sequential displays.

To understand why many previous approaches have not been sufficient in decreasing the response time of LC devices, it is helpful to consider what governs that time. In most LC devices, the director orientation results from the competition between torques exerted by an applied electric field, and the elastic torques resulting from the director are not being uniformly aligned with the surface-imposed orientation. The response time of the device is different for the case of the transition to a more distorted director field with the application of a higher voltage (call this, the voltage-applied transition) than it is to the less distorted director field with the application of a lower voltage (call this, the voltage-removed transition). If we would like to decrease the response time for the first case, an approach is just to apply a higher voltage during the transition, but the response time of the second case is limited by the material properties of the LC material that cannot be chosen at will. Therefore, it is typical that the total response time of a LC device is limited by the time required for transition to the less distorted state when the applied voltage is lowered (or removed).

Therefore, it has been the focus of a great deal of research to modify the material properties of LC materials to decrease the response time. But for many applications, the results of this work have not been sufficient.

Haven<sup>9</sup> has suggested a device modification that solves the problem of having the response time controlled by the voltage-removed transition. He has shown that in a device that consists of two crossed LC cells, that it is possible to have both the optical transition between a state of increased light transmission, and to a state of decreased light transmission be controlled by the response time of the voltage-applied liquid crystal director transition. This is made possible by “optically hiding” the voltage-removed transition by configuring the device, so that it is possible that while the two cells are relaxing together, the net retardation of the device stays zero by having the two cells have the same retardation at each time point during the relaxation.

In this article, we show that it is possible to extend that concept to a device that has grayscale. A device design is presented, where the switching between retardation states of the device is accomplished by increasing the voltages on one of the two paired LC cells. This approach allows for a much faster response than when switching between states is controlled by the elastic relaxation of the LC director field. The device can be used directly as a variable retarder or with polarizers to provide a high-speed multilevel optical attenuator.

## 2 Multilevel LC Device Design and Driving Method

Our multilevel device is based on the shutter device concept of Haven.<sup>9,10</sup> In this section, it is shown that the design of Haven can be extended to a fast-switching retarder and a grayscale LC attenuator. The structure of our fast-response multilevel LC shutter is illustrated in Fig. 1(a). The fast-response multilevel LC attenuator consists of two LC  $\pi$ -cells with their rubbing directions orthogonal to each other. For an attenuator application, the two  $\pi$ -cells are sandwiched between crossed polarizers with rubbing direction of each  $\pi$ -cell at 45 deg to the polarizer absorption axis. For cell A, the rubbing direction of the two substrates is in  $+x$  direction. For cell B, the rubbing direction is in  $+y$  direction. The total phase retardation of two  $\pi$ -cells,  $\varphi_{\text{Total}}$ , is equal to

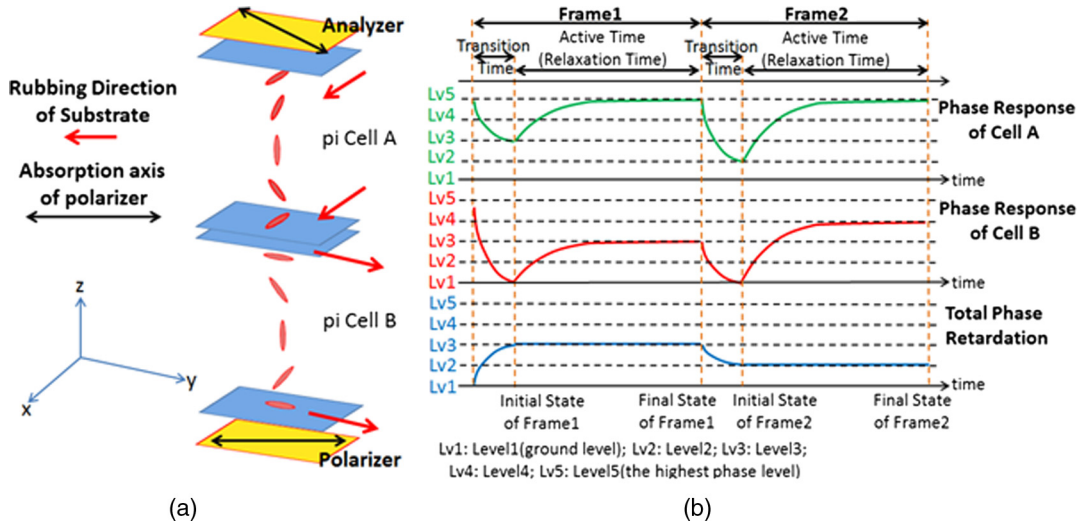


Fig. 1 (a) Structure of grayscale LC attenuator and (b) driving idea of grayscale LC attenuator.

$\varphi_A - \varphi_B$ , where  $\varphi_A$  and  $\varphi_B$  are the phase retardation values of cells A and B, respectively.

The driving scheme of our fast-response multilevel LC attenuator is in Fig. 1(b). The “frame time” is equal to “transition time” plus “active time.” The transition time is the switching time between different levels. The active time is the time that the net retardation level ( $\varphi_{\text{Total}}$ ) is constant. The states of LC  $\pi$ -cells in the beginning and at the end of the active time are called initial state and final state. We will show that, during the active time, the LC director field relaxes to its initial state, so the active time must be longer than the cell relaxation time to allow this to occur. In our method, the transition time is limited by the response time of the LC cell when a voltage is applied, and the active time (relaxation time) is limited by the response time of the LC cell when an applied voltage is removed.

In this article, we use an attenuator with five gray levels of transmission as an example. We define the level 1 state as the lowest phase retardation state, and the level 5 state as the state with the highest phase retardation, as shown in Fig. 1(b).

In the design of an appropriate drive scheme, we use a few basic considerations here: First, we always use a rising voltage to change the state of the  $\pi$ -cells from the final state of previous frame to the initial state of the current frame. So, we always let cell A relax back to the level 5 state, the highest phase retardation state, at the end of each frame. This condition guarantees that we can tune total phase retardation to any level in the next frame by lowering the phase retardation of cell A (by increasing the voltage). Second, in the active time, we need to keep total phase retardation of the two  $\pi$ -cells at a constant value, which is equal to target phase retardation for each frame. And third, to ensure cell B will be able to compensate for cell A during its relaxation to its highest retardation value in the beginning of each active time interval.

Equations (1) to (3) are from the above three conditions.

$$\varphi_B^i = \varphi_{\text{level1}} \quad (1)$$

$$\varphi_A^f = \varphi_{\text{level5}} \quad (2)$$

$$\varphi_A - \varphi_B = \varphi_{\text{Target of frame}} = \text{constant; in active time,} \quad (3)$$

where the superscript  $i$  designates the initial state, and superscript  $f$  is for the final state.

We now would like to show the method for finding the drive voltages versus time. We can know the level of phase retardation of cell A at the initial state as shown in Eq. (4) by combining Eqs. (1) and (3).

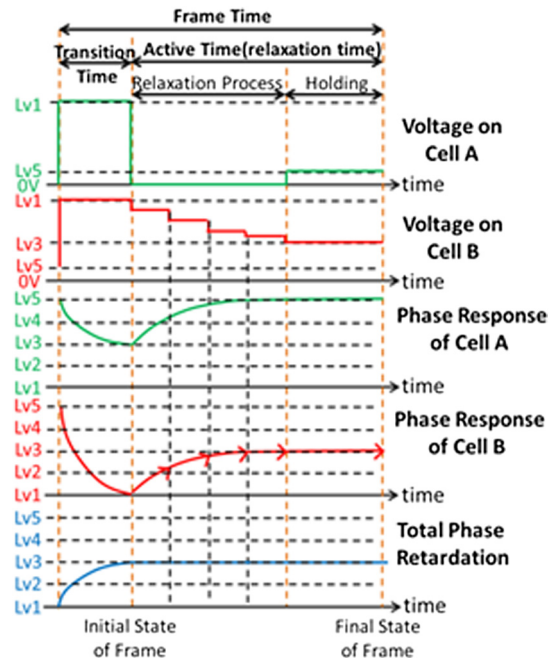
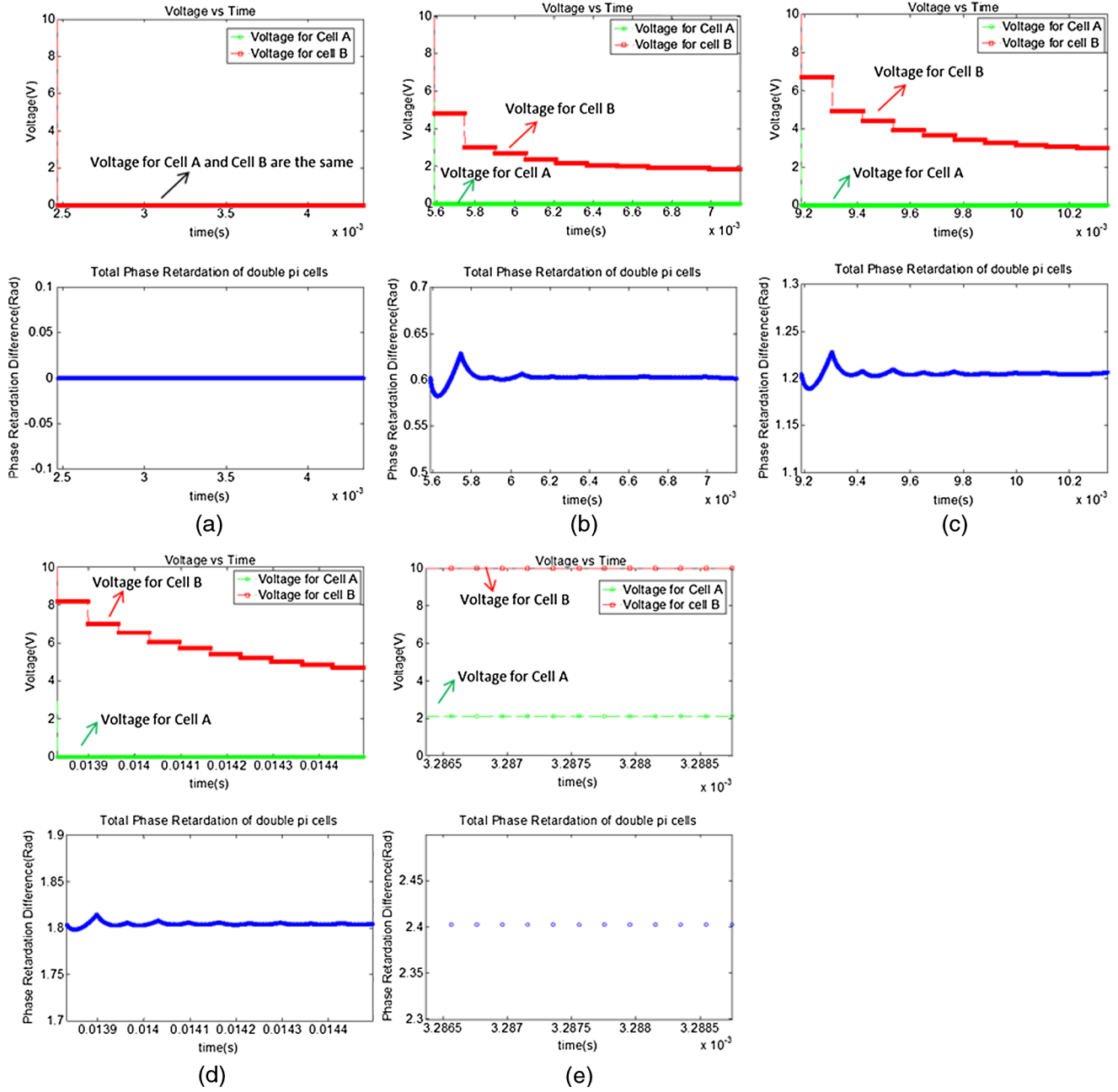


Fig. 2 Voltage and phase retardation of  $\pi$ -cells for illustration of the idea of inserting and holding voltages to keep total phase retardation constant. The total phase retardation (blue curve) is equal to phase retardation of cell A (green curve at third graph) and substrate phase retardation of cell B (red curve at fourth graph).



**Fig. 3** Simulation result of total phase retardation and applied voltage for cells A and B during relaxation process at different gray level frames. In the upper graphs, the green dots and lines are voltage for cell A, and the red dots and lines are voltage for cell B. In the lower graphs, we show total phase retardation (a) for dark frame; (b) for level 2 frame; (c) for level 3 frame; (d) for level 4 frame; and (e) for bright frame. The simulation is used red light (633 nm), and maximum phase retardation can be larger than  $\pi$  for wavelength of blue light (480 nm).

$$\varphi_A^i = \varphi_{\text{Target of frame}} + \varphi_{\text{level}1}. \quad (4)$$

From Eqs. (2) and (3), we can also know phase retardation level of cell B at its final state, as shown in Eq. (5). Knowing the phase retardation levels for two  $\pi$ -cells at initial and final states, we can find out corresponding voltages to drive them.

$$\varphi_B^f = \varphi_{\text{level}5} - \varphi_{\text{Target of frame}}. \quad (5)$$

We use one frame with a target phase retardation of gray level 2 as an example shown in Frame 2 of Fig. 1(b). For simplicity, we can assume that phase retardation of the lowest phase retardation state,  $\varphi_{\text{level}1}$ , equal to 0 and

phase retardation difference between any two adjacent levels is equal to  $\Delta\varphi$ ; so  $\varphi_{\text{level}1} = 0$ ,  $\varphi_{\text{level}2} = \Delta\varphi$ ,  $\varphi_{\text{level}3} = 2\Delta\varphi$ ,  $\varphi_{\text{level}4} = 3\Delta\varphi$ , and  $\varphi_{\text{level}5} = 4\Delta\varphi$ . The target phase retardation,  $\varphi_{\text{Target of frame}}$ , is set up equal to  $\varphi_{\text{level}2}$  and by plugging into Eqs. (4) and (5) we can get

$$\varphi_A^i = \varphi_{\text{level}2} + \varphi_{\text{level}1} = \Delta\varphi = \varphi_{\text{level}2} \quad (6)$$

$$\varphi_B^f = \varphi_{\text{level}5} - \varphi_{\text{level}2} = 4\Delta\varphi - \Delta\varphi = \varphi_{\text{level}4}. \quad (7)$$

However, in relaxation process with overshoot method, speed of relaxation of the different  $\pi$ -cells is different.

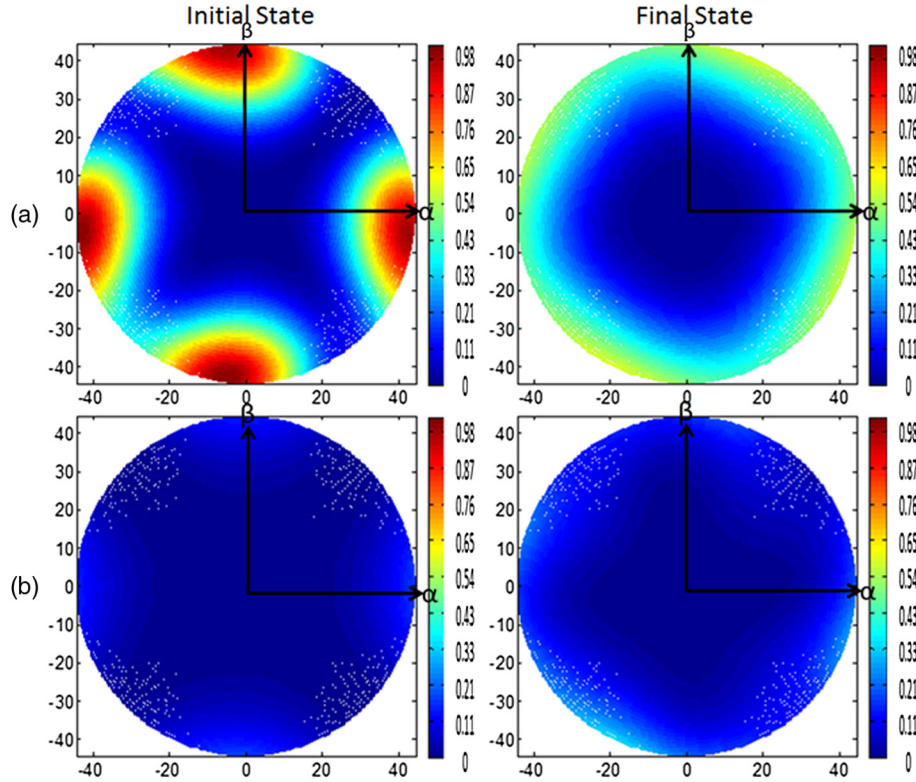


**Fig. 4** Normalized transmission intensity at different viewing angle for dark frame at initial and final states; (a) without compensators; and (b) with Fuji films as compensators; where  $\alpha$  is angle of transmission direction with respect to  $z$  axis in  $x - z$  plane and  $\beta$  is angle of transmission direction with respect to  $z$  axis in  $y - z$  plane.

Relaxation time of cell A is always slower than or equal to cell B, so the total phase retardation will not be constant. To solve this problem, we need to insert voltage points to be applied to cell B to slow down the relaxation speed during relaxation process. The idea is illustrated in Fig. 2.

As a result, we can keep total phase retardation constant during the relaxation process in the active time.

### 3 Simulation and Experiment Approach

#### 3.1 Simulation Approach

By minimizing free energy, we can know equilibrium state of  $\pi$ -cell at different voltages, so we use the Frank free energy [Eq. (8)] and the Euler-Lagrange equation [Eq. (9)] to calculate the director distribution of the  $\pi$ -cells.<sup>11</sup>

$$f_{\text{Total}} = 1/2\{K_{11}(\nabla \cdot n)^2 + K_{22}[n \cdot (\nabla \times n) - q_0]^2 + K_{33}[n \times (\nabla \times n)]^2\} + (-1/2\vec{D} \cdot \vec{E} + \text{constant}) \quad (8)$$

$$-\gamma \frac{\delta\theta}{\delta t} = \frac{\delta f_{\text{Total}}}{\delta\theta} - \frac{d}{dz}(\delta f / \delta\theta') = 0; \theta' = \frac{\delta\theta}{\delta z};$$

$$-\gamma(\sin\theta)^2 \frac{\delta\phi}{\delta t} = \frac{\delta f}{\delta\phi} - \frac{d}{dz}(\delta f_{\text{Total}} / \delta\phi') = 0; \phi' = \frac{\delta\phi}{\delta z}, \quad (9)$$

where  $q_0 = 2\pi/p_0$  is spontaneous twist,  $K_{11}$ ,  $K_{22}$ , and  $K_{33}$  are the splay, twist, and bend elastic constants,  $D$  is electric displacement,  $E$  is electric field,  $\gamma$  is viscosity,  $\theta$  is polar angle,  $\phi$  is azimuthal angle, and  $z$  is the position in the

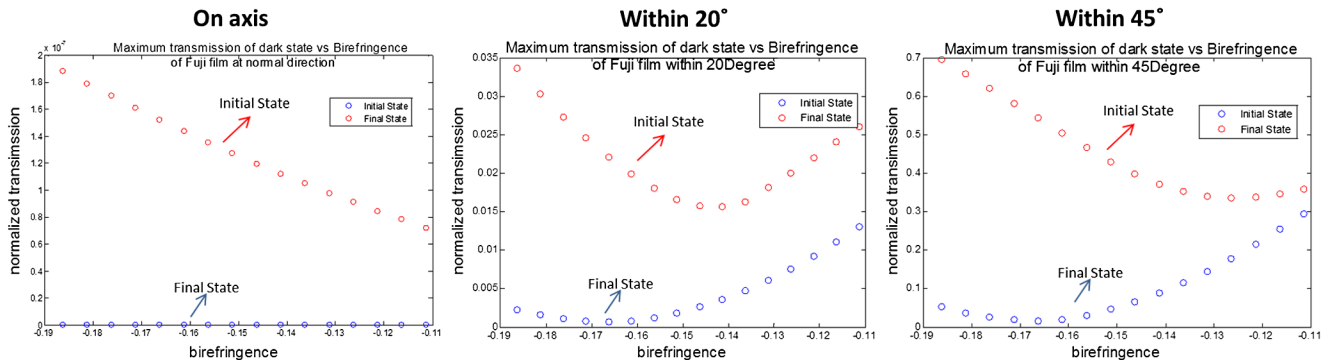


**Fig. 5** Simulation result of maximum normalized transmission with different birefringence of Fuji films as compensator at different range of viewing angle for dark frame. Maximum transmission of bright state is 1.

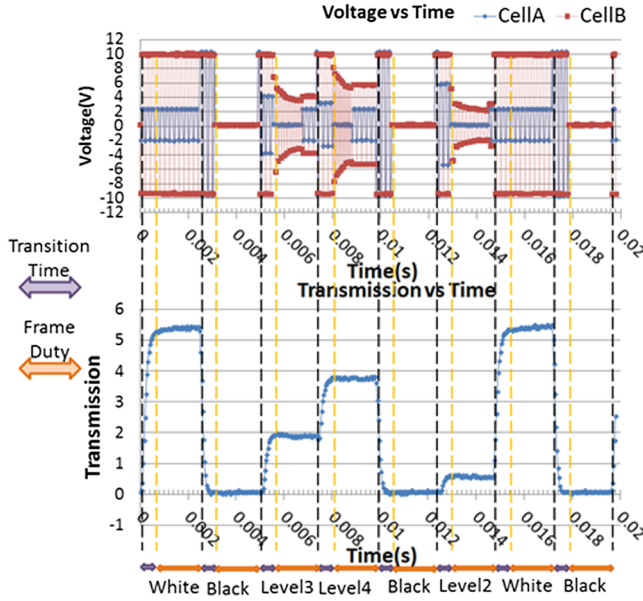


**Fig. 6** Transmission and applying voltages for our fast-response display when it shows different gray level frames sequentially. The upper graph is applied voltage for cells A and B. The lower graph is transmission intensity at different times.

layer (between 0 and  $d$ , where  $d$  is the layer thickness). We set up the initial condition of our  $\pi$ -cell in twist state and separate our LC  $\pi$ -cell to 201 layers.

The LC we used in the experiments is MLC 6080, and the parameters we use in the simulation are: cell thickness is  $4.95 \mu\text{m}$ ; wavelength of light  $\lambda = 633 \text{ nm}$ ;  $\epsilon_0 = 8.85 \times 10^{-12} \text{ C}^2/\text{Nm}^2$ ; dielectric anisotropy  $\Delta\epsilon = 7.4$ ; viscosity  $\gamma = 0.0397 \text{ Pa}\cdot\text{S}$ ;  $K_{11} = 14.4 \times 10^{-12} \text{ N}$ ;  $K_{22} = 7.1 \times 10^{-12} \text{ N}$ ;  $K_{33} = 19.1 \times 10^{-12} \text{ N}$ ; ordinary refractive index<sup>12</sup>  $n_o = 1.50027$ ; birefringence<sup>12</sup>  $\Delta n = 0.18633$ ; pretilt angle is 4.4 deg; and operation voltage is 0 to 10 V.

The steps of our simulation are: First, we pick five retardation levels for our simulation and the corresponding voltage for these five levels. Then, we calculate the phase retardation,  $\varphi$ , of  $\pi$ -cell from director distribution at different voltages by Eqs. (10) and (11).

$$\Delta n_{\text{eff}}(z) = \frac{n_e n_o}{\sqrt{n_e^2 \sin^2[\theta(z)] + n_o^2 \cos^2[\theta(z)]}} - n_o \quad (10)$$

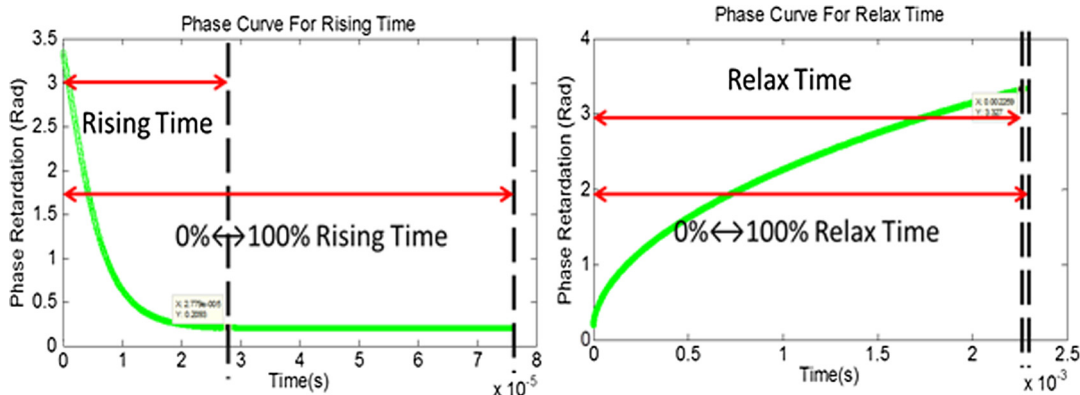


**Fig. 7** Phase response of  $5.8\text{-}\mu\text{m}$   $\pi$ -cell, which is used for fast-response multilevel liquid crystal (LC) shutter that is optimized for 633 nm (red light) application.

$$\varphi = \int_0^d \frac{2\pi}{\lambda} \Delta n_{\text{eff}}(z) dz, \quad (11)$$

where  $n_{\text{eff}}$  is effective birefringence.

Second, we apply voltages to set the director distribution of the  $\pi$ -cells to provide the phase retardation needed for the initial state. Third, we simulate relaxation process of cell A with overshoot method to know how much time we need for relaxation process. Next, we simulate relaxation process of cell B in 10 equal time-length steps. In each step of the relaxation process of cell B, we find the voltage that keeps the total phase retardation constant.

### 3.2 Experiment Approach

We made two  $\pi$ -cells with  $5\text{-}\mu\text{m}$  spacers and filled with the LC, MLC 6080, from Merck. We measure transmission intensity of  $\pi$ -cells at different voltages under crossed and parallel polarizers to acquire voltage versus phase retardation data by Eqs. (12) and (13).<sup>13</sup>

$$I_{\perp} = I_0 \sin^2(\varphi/2) \quad (12)$$

$$I_{\parallel} = I_0 \cos^2(\varphi/2), \quad (13)$$

where  $I_0$  is incident light intensity,  $\varphi$  is phase retardation,  $I_{\perp}$  and  $I_{\parallel}$  are transmission intensity under crossed and parallel polarizers, respectively.

We measure rising time from level 5 state to level 1 state and relaxation time from level 1 state to level 5 state with overshoot method to determine the maximum transition time and active time of our device.

We modify the value of applied voltage for cell B obtained from the simulation result to minimize divergence of transmission intensity from desired transmission during relaxation process for different gray level frames.

## 4 Results and Discussion

### 4.1 Simulation Result

An issue with our fast retarder design is the ability for the retarder to hold the desired value as the cell's director configurations are changing. Figure 3 shows the total phase

retardation and value of applied voltage for cells A and B during relaxation process. The maximum phase retardation for bright state could be larger than  $\pi$  for blue light (480 nm) application. For the case of the variable retarder being used as an optical shutter, it is the variation in transmission as defined by Eq. (13) that is an issue. We quantify the deviation from the desired transmission in an active time interval by the quantity  $\eta_{\text{error}}$ . The definition of  $\eta_{\text{error}}$  is shown in Eq. (14).

$$\eta_{\text{error}} = I_{\text{max deviation}}/I_{\text{target}} \times 100\%, \quad (14)$$

where  $I_{\text{max deviation}}$  is the maximum transmission difference between the target transmission ( $I_{\text{target}}$ ) for the frame and the actual transmission. We calculate divergence of transmission intensity  $\eta_{\text{error}}$  for gray level 2 to gray level 4 is not larger than 8.78%.

Another issue with this device is the effect of the angle of illumination on the retardation. If the retarder is used as a high-speed optical shutter, this issue becomes most significant when considering the dark state transmission. The transmission of the dark frame in the initial state (both cells at retardation level 1) and final state (both cells at retardation level 5) for different light transmission angles is shown in Fig. 4(a).

Figure 4(a) shows a significant amount of light leakage for light angles larger than 30 deg from the cell normal. It has been shown<sup>14</sup> that passive optical compensators that are a multilayer negative C plate with optic-axis direction corresponding to the LC director in the lowest retardation state of the device can be used to reduce this leakage. However in this case, unlike that previously discussed, we expect the optimum value of the compensator chosen will be different for the initial and final states of the device, and we need to search for the a compromise design of the compensator.

In Fig. 5, we summarize the information of graphs like that shown in Fig. 4(b), for different values of the material birefringence of the splayed compensator design of Mori and Bos.<sup>14</sup> We used four compensators in the simulation, where the thickness of each film is equal to half thickness of the LC  $\pi$ -cells. The graphs in Fig. 5 show the maximum transmission of the dark state frame in the initial and final states with the compensator films. We show three different ranges for the angle of transmission direction with respect to the cell normal. The maximum transmission in the dark frame means the highest transmission observed in graphs, as shown in Fig. 4, within the polar angles given. It can be seen that to have the best dark state within 45 deg, we can use the splayed compensator films with material birefringence equal to  $-0.1263$ , because it provides the minimum transmission of the final state, which is the state of the greatest leakage. The transmission at different detecting angles of the LC optical retarder for the dark frame at initial and final states with splayed compensation films whose birefringence is  $-0.1263$  is shown in Fig. 4(b). The off-axis light leakage is shown to be considerably improved over the case of no compensators.

## 4.2 Experimental Result

In Fig. 6, we show applied voltages of cells A and B and transmission at different times for our fast-response

multilevel optical attenuator when it operates with eight different frames sequentially. For this example, we choose eight target levels to be: white (level 5), black (level 1), level 3, level 4, black (level 1), level 2, white (level 5), and black (level 1) sequentially. The transmission is almost constant during the active times, even though the cells are relaxing during these times. The active time in this example is 1.8 ms, and transition time is 0.65 ms. In the example simulation result, by using three steps in the relaxation for level 4 frame, the  $\eta_{\text{error}}$  is about 3.5%.

## 4.3 High-Speed Multilevel Retarder

Because the transition time between retardation levels, or transmission levels, is controlled by the electric field term of Eq. (8), they are approximately proportional to the square of the applied voltage. So while 10 V was used in the above example, a 50-V drive would be expected to reduce the transition time by a factor of 25.

Figure 7 shows the phase response for rising and relaxing voltages for 5.8- $\mu\text{m}$   $\pi$ -cell, which is used for LC retarder optimized for red light (633 nm). In this case, we see that the voltage-applied transition time is approximately 28 ms.

## 5 Conclusion

We have shown a design for a fast-response multilevel LC retarder whose switching time is only about 28  $\mu\text{s}$  with 50 V operation voltage, while using obtainable LC materials. The fast-response multilevel LC retarder has a minimum active time that is equal to the relaxation time of the used LC cells that was shown in an example to be 2.20 ms. The device has the potential to be used as intensity modulator in optical communications or field sequential 3-D displays.

## References

1. S. G. Kim et al., "Stabilization of the liquid crystal director in the patterned vertical alignment mode through formation of pretilt angle by reactive mesogen," *Appl. Phys. Lett.* **90**(26), 261910 (2007).
2. C.-H. Pai et al., "Fast-response study of polymer-stabilized VA-LCD," *J. Soc. Inf. Display* **18**(11), 960-967 (2010).
3. D. K. Yang, L. C. Chien, and J. W. Doane, "Cholesteric liquid crystal/polymer dispersion for haze-free light shutters," *Appl. Phys. Lett.* **60**(25), 3102-3104 (1992).
4. B.-G. Wu, J. H. Erdmann, and J. W. Doane, "Response times and voltages for PDLC light shutters," *Liq. Cryst.* **5**(5), 1453-1465 (1989).
5. P. J. Bos and K. R. Beran, "The pi-cell—a fast liquid-crystal optical-switching device," *Mol. Cryst. Liq. Cryst.* **113**(1-4), 329-339 (1984).
6. F. S. Y. Yeung and H. S. Kwok, "Fast-response no-bias-bend liquid crystal displays using nanostructured surfaces," *Appl. Phys. Lett.* **88**(6), 063505 (2006).
7. Y. K. Jang and P. Bos, "Optimization of the white state director configuration for perfectly compensated Pi-cell devices," *Jpn. J. Appl. Phys.* **46**(9A), 5821-5828 (2007).
8. L.-Y. Wang et al., "Improvement of fast response LC materials by Bent-core dopants in optical compensated bend (OCB) mode liquid crystal displays," *SID Symp. Dig. Tech. Pap.* **39**(1), 40-43 (2008).
9. T. J. Haven, "A liquid-crystal video stereoscope with high extinction ratios, a 28 % transmission state, and one hundred-microsecond switching," *Proc. SPIE* **761**, 23-26 (1987).
10. J. Osterman and T. Scheffer, "Contrast-enhanced high-speed polarization modulator for active-retarder 3D displays," *SID Symp. Dig. Tech. Pap.* **42**(1), 93-96 (2011).
11. X. H. Wang et al., "Finite-difference time-domain simulation of a liquid-crystal optical phased array," *J. Opt. Soc. Am. A* **22**(2), 346-354 (2005).
12. W. M. Jones et al., "Polarization-independent modulation for projection displays using small-period LC polarization gratings," in *International Display Research Conference*, Vol. 26, (2006).
13. P. Yeh and C. Gu, *Optics of Liquid Crystal Displays*, Wiley, Hoboken, NJ (1999).

14. H. Mori and P. J. Bos, "Optical performance of the pi cell compensated with a negative-birefringence film and an a-plate," *Jpn. J. Appl. Phys.* **138**(Part 1, No. 5A), 2837–2844 (1999).



**HsienHui Cheng** is a PhD student in the Liquid Crystal Institute at Kent State University, Kent, Ohio. He is currently involved in research related to nonmechanical fast response and beam steering devices. He has a BS degree from the Physics Department of National Dong Hua University, Hualien city and an MS degree from the Physics Department of National Cheng Kung University, Taiwan.



**Achin Bhowmik** is the director of perceptual computing at Intel Corporation, Santa Clara, California, where he leads the development of next-generation computing solutions based on natural human interfaces and visual computing technologies. Previously, he led the advanced video and display technology group, responsible for developing power-performance optimized multimedia processing technologies for Intel's computing products. His prior work includes develop-

ment of high-definition display systems based on all-digital liquid-crystal-on-silicon microdisplay technology, fast electro-optic modulation in organic molecular crystals, and integrated optoelectronic circuits for

high-speed communication networks. As an adjunct professor, he has taught graduate-level courses on computer vision, image processing, and display technology. He has >100 publications, including a book and 25 issued patents. He is an associate editor for the *Journal of the Society for Information Display*. He has been a session chair and invited and keynote speaker at a number of major conferences. He is on the board of directors for OpenCV, the organization behind the open-source computer vision library.



**Philip J. Bos** is a professor of chemical physics and associate director of the Liquid Crystal Institute at Kent State University, Kent, Ohio. Before joining Kent State in 1994, he was a principle scientist in the Display Research Laboratory of Tektronix Inc. He received his PhD in physics from Kent State in 1978. He has authored over 100 papers in the field of liquid crystals and liquid crystal displays and has over 25 issued patents. His field of interest is applica-

tions of liquid crystals with contributions to fast liquid crystal electro-optical effects including the invention of the pi-cell. He is active in the field of displays and was twice the general chair of the International Display Research Conference. He is a fellow of the SID and has received the Distinguished Scholar Award from Kent State University. Please see <http://www.lci.kent.edu/PI/BosP.htm>.